Available online at www.sciencedirect.com

ScienceDirect

Procedia Manufacturing 34 (2019) 186–192

Procedia MANUFACTURING

www.elsevier.com/locate/procedia

47th SME North American Manufacturing Research Conference, Penn State Behrend Erie, Pennsylvania, 2019

Applying ultrasonic vibration during single-point and two-point incremental sheet forming

Randy Cheng[a*], Nicholas Wiley[b], Matt Short[b], Xun Liu[c], Alan Taub[a,d]

[a]*Department of Materials Science & Engineering, University of Michigan, Ann Arbor, MI USA*
[b]*Edison Welding Institute, Columbus, OH USA*
[c] *Department of Materials Science & Engineering, The Ohio State University, Columbus, OH USA*
[d] *Department of Mechanical Engineering, University of Michigan, Ann Arbor, MI USA*

* Corresponding author. Tel.: 1-404-483-7554 *E-mail address:* randyjfc@umich.edu

Abstract

Ultrasonic assisted (UA) deformation has been studied on a variety of materials in both fundamental tensile and compression tests as well as in relevant industrial processes. Reductions in flow stress are a common observation when applying UA during material plastic deformation. The objective of this work is to study the effects of ultrasonic energy on single-point (SPIF) and two-point (TPIF) incremental forming. A longitudinal ultrasonic vibration is applied to a hemispherical ISF tool at 20kHz oscillating frequency. A series of conical shapes were selected for UA-SPIF and a 45° conical shape backing die is selected for UA-TPIF. Generally, a positive correlation between oscillation amplitude and reduction in forming forces is observed in the investigated conditions. The force reduction in UA-TPIF is much more significant compared with UA-SPIF. It is hypothesized that UA-SPIF allows membrane vibration of the entire sheet, which lowers the effective ultrasonic energy input into the local plastic deformation region. In addition, UA-TPIF shows a local sheet thickness reduction in regions where ultrasonic oscillation is applied.

Keywords: Single-point incremental sheet forming, Two-point incremental sheet forming, Ultrasonic assistance, Ultrasonic vibration, Aluminum, Forming force

1. Introduction

This study investigates the effects of applying ultrasonic vibration during the incremental sheet forming (ISF) process. ISF is a sheet fabrication technology that can produce free-form surfaces incrementally, often requiring no dies. The complex stress state developed during ISF stabilizes the material and suppresses necking, which significantly enhances the sheet forming limit compared with conventional forming operations such as stamping and hydroforming [1, 2]. During the process, the sheet periphery is clamped in a blank holder. A generic tool, usually with a hemispherical end, is applied to locally deform the sheet with a predefined toolpath. The final desired geometry is achieved progressively. Based on different configurations as shown in Fig. 1 [3], the ISF process can be classified into three main categories. First is single point incremental forming (SPIF), where no die is needed and only one generic tool is required, as shown in Fig. 1(a). Second is two-point incremental forming (TPIF), where a partial or a full die is utilized, as shown in Fig. 1(b). Due to the actual physical constraint of the die, the clearance between tool tip and the die surface needs to be adjusted to accommodate the final desired thickness of the deformed sheet. Accordingly, an additional parameter of squeeze factor is introduced, and the detailed definition is provided in the following section. The third category is double sided incremental forming (DSIF), where an additional

10.1016/j.promfg.2019.06.137

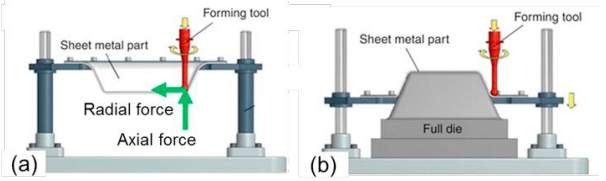

supportive tool is kinematically applied at the bottom side of the sheet, as shown in Fig. 1(c). A typical spiral toolpath for forming a cone shape is shown in Fig. 1(d).

Fig. 1 Schematic illustration of the incremental forming process: (a) single point incremental forming SPIF and (b) two-point incremental forming TPIF [3]

Ultrasonic vibration has been applied in various manufacturing processes and shown to offer multiple benefits. Baghlani et al. [4] performed ultrasonically assisted deep drilling of an Inconel superalloy and showed increased material removal rate, reduced drilling force and improved surface roughness. Similar benefits were also observed in other machining processes, such as turning [5] and milling [6]. In addition, ultrasonic energy has been utilized in improving several traditional forming technologies, including wire drawing [7], deep drawing [8], upsetting [9] and extrusion [10]. In these processes, ultrasonic vibration of the corresponding forming tool modifies the surface frictional behavior and also transfers the energy into the bulk material with reports of reduced forming forces [11]. The influence of ultrasonic vibration on the frictional behavior depends on the relative direction between the vibration and sliding motion. When the ultrasonic motion is parallel to the tool sliding direction, reduction of friction force is more effective than the perpendicular direction [12]. When ultrasonic vibration is applied in the same plane as the material-tool contact surface, the tendency of slipping compared with sticking increases in the dynamic frictional condition. The induced elastic-plastic deformation of surface asperities enhances movement of the hills into the valleys. As a result, the friction resistance can be reduced [9, 13, 14] with improved surface finish quality [15]. Amini et al. [16] and Vahdati et al. [17] fabricated an attachment to the chuck of a CNC machine that can introduce longitudinal ultrasonic vibration and rotary motion during SPIF process. A simple groove geometry was formed on aluminum 1050 sheet. Increased formability and reduced forming force were reported under the assistance of ultrasonic vibration.

Ultrasonic softening was first discovered in 1955 [18] by Blaha and Langenecker, where a remarkable reduction in the flow stress was observed immediately when a high frequency vibration was applied during plastic deformation of zinc. This softening effect was later shown in various alloys when they were subjected to combined quasi-static and oscillatory stress, with the frequency in range of 20-100kHz and amplitude around 1-10μm [11]. The reduction in yield strength is generally independent of ultrasonic frequency in the range of 15-80kHz [19, 20]. The softening occurs temporarily while the vibration is applied. After the vibration is stopped, there can be either residual hardening or softening, depending on the material [21-23]. Depending on the material systems, reduction of the deformation stress can be proportional to the ultrasonic vibration amplitude [24] or acoustic intensity [19, 25], which is proportional to the square of the amplitude.

The fundamental physical principles governing the softening phenomenon are still being investigated. Proposed theories in the literature generally fall into two categories. One is referred to as acoustic softening, which describes the direct interaction between ultrasonic vibration and dislocation movement. The acoustic energy is preferentially absorbed by localized lattice imperfections, such as vacancies, dislocations and grain boundaries. This increases the mobility of dislocations and reduces the critical resolved shear stress [26]. In addition, ultrasonic vibration was also reported to internally alter the material microstructures. Siu et al. [27] observed that subgrain formation was extensively enhanced during ultrasonically assisted micro-indentation tests of aluminum. The dislocation dynamics simulation showed enhanced dipole annihilation as one of the underlying mechanisms [28]. Dutta et al. [29] performed ultrasonically assisted tensile tests on low carbon steel and noticed that both dislocation density and the fraction of low-angle grain boundaries decreased. The subgrain formation was reduced, which was unlike the findings of Siu et al. [27] and was explained based on the different deformation mechanisms between FCC and BCC metals. Lum et al. [22] reported dynamic annealing effects from ultrasonic vibrations. An alternative proposed theory for ultrasonic softening is pure stress superposition, which assumes that fundamental plastic behavior of the material remains unchanged. Material deformation resistance is governed by the addition of static and high frequency alternating loads [30-32]. The ultrasonic softening can also be a coupled result of both acoustic softening and stress superposition, as shown by a combined model and experimental analysis from Daud et al. [33]. The combination is usually referred to as the acousto-plastic effect (APE) [11].

In this study, the ultrasonic effect on both single-point and two-point ISF is analyzed and compared for three forming geometries under various conditions, where the vibration is applied along the longitudinal axis of the forming tool during the process.

2. Experiments

A schematic illustration of the ultrasonically assisted SPIF system is shown in Fig. 2(a). The ultrasonic vibration is applied longitudinally along the axis of the incremental forming tool with an ultrasonic tool holder. The ceramic piezoelectric transducers are integrated inside the device and the electric power supply is connected through the center of the spindle. The vibration amplitude of the tool is adjusted by the output power of the ultrasonic generator. The tool length protruding from the spring collet directly affects the resonant oscillating frequency of the device. Using an oscilloscope, the resonant frequency can be observed with respect to the tool protrusion length. The tool extends 127mm out of the collet and is tuned to be half of the ultrasonic vibration wavelength at a resonant

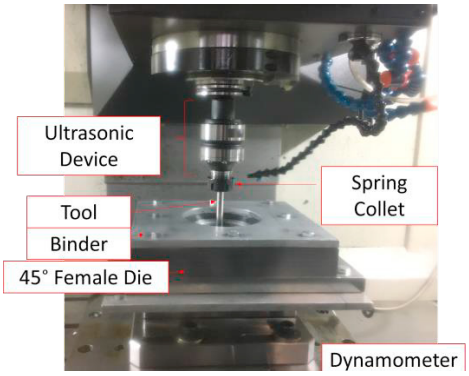

Fig. 2 Image of the ultrasonic TPIF system

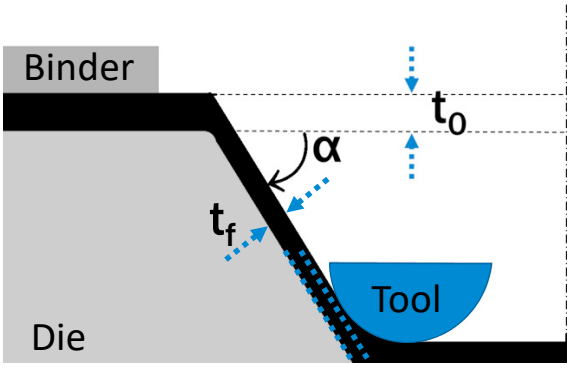

Fig. 3 Schematic of forming angle and squeeze

Table 1 Summary of investigated UA-ISF conditions and their corresponding axial and planar force reductions

Process	Shape	Step Size (mm)	Squeeze Factor (%)	Ultrasonic Amplitude (μm)	Axial Force Reduction (%)	Planar Force Reduction (%)
SPIF	45°cone	0.50	N/A	0, 4.52	4.7	5.5
	67° cone	0.50	N/A	0, 1.66, 2.48, 3.29, 4.11	0, 0.9, 1.8, 4.1, 6.9	0, 1.5, 2.5, 4.1, 7.5
	25°- 84° Funnel	0.50	N/A	0, 1.66, 2.48, 3.29	0, 3.1, 2.5, 5.2	0, 2.7, 2.4, 4.2
TPIF	45°cone	0.50	0, 40	3.29	11	15
		0.25	40	3.29	18	16

frequency of approximately 20kHz, such that the tool tip is an antinodal point where the maximum amplitude of vibration occurs. The amplitude values were measured using a laser vibrometer on the unloaded tool under different levels of power output from the ultrasonic generator. The value of amplitude vibration reported is that of the unloaded tool. The tool has a diameter of 12.7mm and a hemispherical end. The actual experimental setup for the ultrasonically assisted SPIF is shown in Fig. 2(b). A dynamometer is mounted below the blank holder to measure the forming force during the process. For ultrasonically assisted TPIF, a 45° cone-shaped female die was used [34, 35].

The workpiece material is Al 7075, O-tempered with a thickness of 1.57mm. A layer of MoS2 grease was spread across the top of the sheet and on the die, when applicable, before all experiments. As compared to our prior work [34, 35] which used a freely rotating spindle, the milling machine used in this study required a minimum spindle rotation speed of 15 revolutions per minute (rpm) which was applied throughout all tests. The toolpath is spiral with a step size of 0.5mm, which is the increment of forming depth for each pass, as shown in Fig. 1(d). Other details of the investigated experimental conditions are summarized in Table 1. In SPIF, the final sheet thickness can be predicted, geometrically, using the sine law as shown in Fig. 3 [36]:

$$t_f = t_0 * \sin(90 - a) \quad (1)$$

By restricting material flow and assuming conservation of volume, the original material with a thickness t_0, would thus elongate and have a thickness correlated to the forming angle α. For TPIF, the squeeze factor δ, which represents the relationship between the deformed sheet thickness and tool-die clearance, is defined with the following equation [36]:

$$\delta = 1 - \frac{d_c}{t_f} = 1 - \frac{d_c}{t_0 cos\ \alpha} \quad (2)$$

Where t_0 is the initial thickness, t_f is the deformed sheet thickness from sine law, α is the wall angle, d_c is the clearance between the tool and die surface in the normal direction as shown in Fig. 3. A value of 0% squeeze factor implies that the sheet just touches the bottom die during forming without further squeezing the sheet.

For SPIF, both the 45° and 67° cones were formed to a depth of 50mm. SPIF funnels were formed to a depth of 68.5mm starting at a 25° angle and ending at 84° with a frame opening of 159mm [37]. The standard dynamometer sampling frequency in the tests was 10Hz. Average force reduction percentages were calculated by taking the difference of the non-UA and UA force values at equivalent time stamps and averaging them.

For TPIF tests, a 45° female die was utilized. In the forming condition of 40% squeeze and 0.5mm step size, the ultrasonic vibration was applied midway during the process. In the condition of 40% squeeze and 0.25mm step size, ultrasonic assistance was cycled on-and-off during the process to study the transient behavior. 3-dimensional scans of the formed parts were obtain using a Hexagon Laser Scanning tool to determine the part thickness.

3. Results

3.1 UA-SPIF

As shown in Fig. 4, two 45° SPIF parts were formed: one without UA and one with an ultrasonic vibration amplitude of 4.52µm. The force reduction was calculated as the percent reduction of the difference between the non-UA and UA samples. The axial and planar average force reduction was calculated to be approximately 4.7% and 5.5% respectively. Looking at the axial forces, repeating regions of gradual reductions in stress are observed. This test was repeated twice and the results were found to be consistent.

Fig. 5 displays the ultrasonic effect during SPIF of a 67° cone with increasing oscillation amplitudes. To better visualize effects of increasing amplitude, a moving mean smoothing function was applied to increase the signal-to-noise ratio of the original data using a 10-point sliding window. As the vibration amplitude increases, a larger reduction in axial forming forces can be observed. A monotonically increasing relationship between the input amplitude and resultant force reduction is seen.

Fig. 6 shows the effect of increasing amplitude on forming force for a funnel with increasing angle. The tool starts with the position on a 25° angle and approaches 84° at the depth of 68.5mm. In all the funnel trials, the sheet exhibited failure at an angle between 80-84° which is to be expected due to the forming limit of ISF. The effect of ultrasonic assistance is small from 25° to 34°. From 34° to 84°, the forming forces begin to decrease. Fig. 6 shows the average force reduction percentage from 100s to 450s for the UA-SPIF funnel. The force reductions for UA-SPIF 45° and 67° cones are also presented in Fig. 7. At a vibration amplitude of 3.29µm, the force reduction almost doubles that of 1.66µm amplitude. Additional experiments are required to understand the break in the positive correlation trend for the 2.48µm oscillation amplitude.

3.2 UA-TPIF

Fig. 8 shows the forming forces for an SPIF, TPIF, and a UA-TPIF sample. The SPIF and zero-squeeze TPIF curves differ initially due to the unconstrained bending region in SPIF [35]. However, the forming forces of the SPIF and zero-squeeze factor TPIF converge to about the same value after about 350 seconds as expected for zero-squeeze factor. The 110N force difference between the 0% and 40% programmed squeeze factor is a result of squeezing between the sheet and

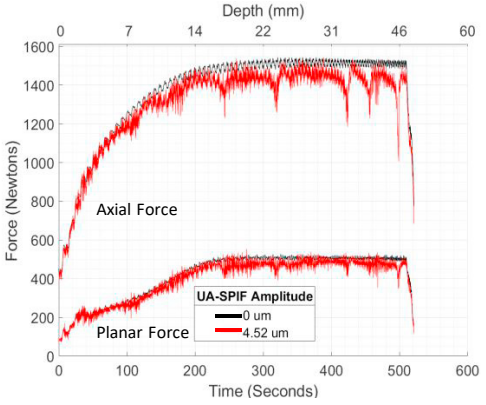

Fig. 4 Forming force comparison between non-UA and UA-SPIF 45° cone

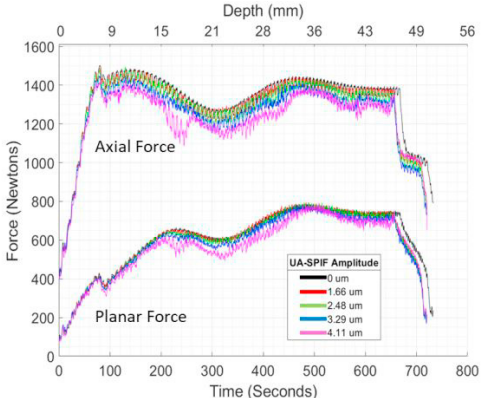

Fig. 5 Forming forces for UA-SPIF 67° cone with varying ultrasonic amplitude

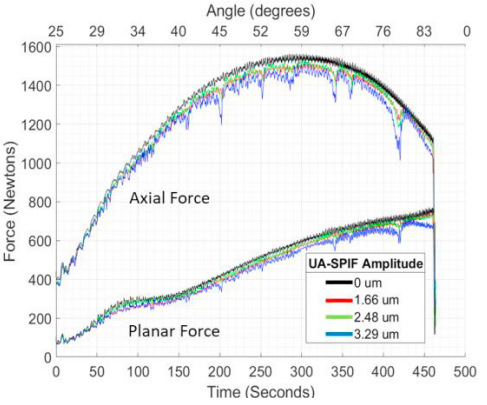

Fig. 6 Forming forces for UA-SPIF funnel with varying ultrasonic vibration amplitude

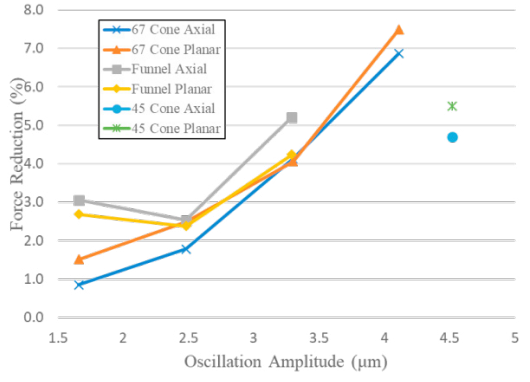

Fig. 7 Force reduction percent for UA-SPIF samples with respect to ultrasonic vibration amplitude

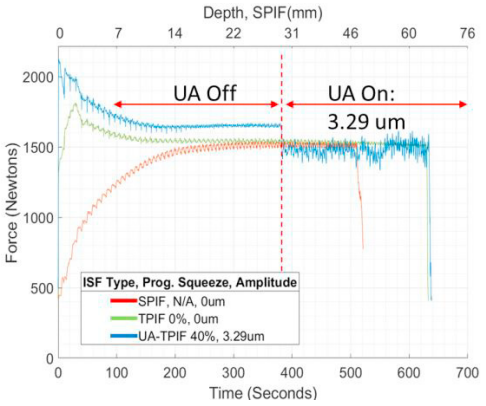

Fig. 8 Axial forming force for a 45° cone comparing SPIF, TPIF, and UA-TPIF with 40% programmed squeeze and 0.50mm step size. Since SPIF, TPIF, and UA-TPIF all have different tool paths, different depth-time profiles are generated. The depth profile represents the SPIF sample.

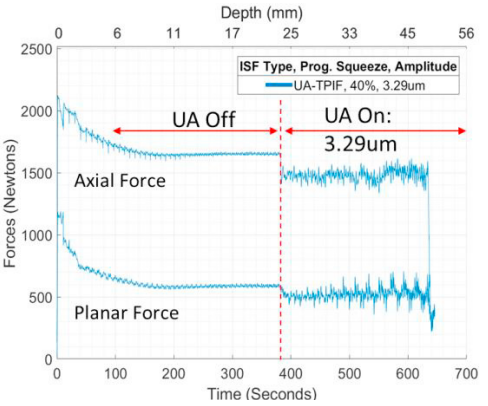

Fig. 9 Axial and planar forces for UA-TPIF 45° cone and 0.50mm step size.

die. At 40% squeeze factor, a superimposed ultrasonic oscillation of 3.29µm was applied at 380 seconds. The axial force shows a distinct drop at 380s and asymptotes to a mean force lower than that in the SPIF and TPIF samples. Both axial and planar forces for the 40% squeezed part are shown in Fig. 9. The average axial and planar force reduction percent is calculated to be approximately 11% and 15% with respect to forces prior to ultrasonic assistance.

Fig. 10 shows the results of a 45° cone at 0.25mm step size and 40% squeeze factor with UA cycled on (regions R2 and R4) and off (regions R1, R3, and R5). The axial and planar force behavior is similar to Fig. 9. The axial forming force drops when UA is turned on and reaches a steady state value. The planar force also experiences a reduction but in a more gradual nature. In both cases, the force experiences a transient when UA is applied and when UA is turned off as seen in regions R2 and R3.

A macroscopic image and 3D thickness color plot of the UA-TPIF part is presented in Fig. 11. Ultrasonic assisted regions are clearly visible with a decreased thickness. A cross section taken along the center of the sample is plotted along with the force curve in Fig. 10. The thickness at the end of region R1 is approximately 1.12mm and the minimum thickness measured in region R2 is 0.97mm. Once UA is turned off, (region R3), a gradual increase in thickness is observed. This transient behavior is repeated with regions R3 and R4. As seen in Fig. 11, regions with UA off are more reflective than regions with UA on.

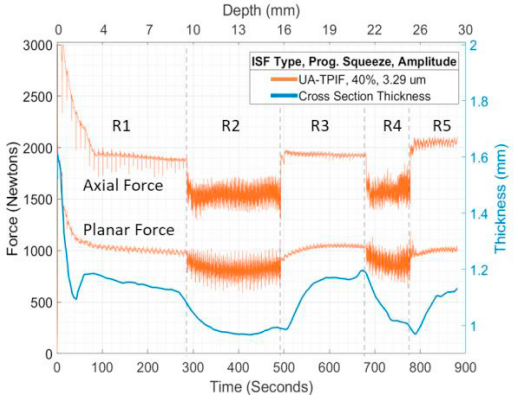

Fig. 10 UA-TPIF forming force and thickness for a 45° cone with 40% programmed squeeze and 0.25mm step size

4. Discussion

4.1 Effect of ultrasonic vibrations on single-point incremental forming

Ultrasonic assisted incremental forming was shown to reduce the forming forces during both single and two-point incremental forming processes. The force reduction magnitude in UA-TPIF is significantly larger than in UA-SPIF as seen in Table 1. From Fig. 4 and Fig. 6, large dips in forces are observed at repeatable stamps in time regardless of the ultrasonic amplitude. Since the frequency of the tool is maintained, we hypothesize that the dips in forces are due to membrane vibration [38]. Without a rigid surface backing the sheet, the forming area of the sheet is unrestrained from vibrating elastically. Thus, a significant amount of acoustic energy is transferred into the elastic vibration of the entire sheet, which reduces the ultrasonic softening effect that would

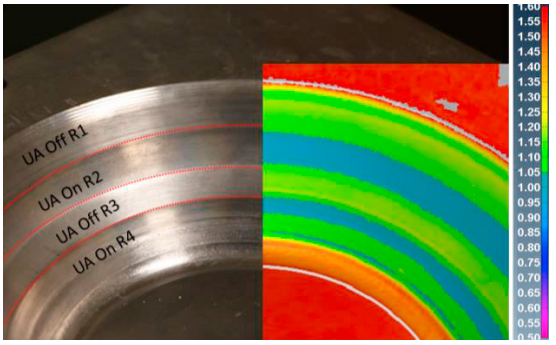

Fig. 11 Macro image of part and 3D thickness color plot in mm

be observed during plastic deformation. During TPIF, this motion is better restrained by the rigid supporting die and allows for more of the acoustic energy to be transferred into plastic deformation and ultimately higher force reduction.

Simplified groove forming UA-SPIF experiments were conducted by Vahdati et al. [17] which displayed force reductions of 23.5%-26.3% at a tool vibration frequency of 21kHz. For an oscillation amplitude of 7.5μm, the force reductions are 3-4 times the values observed here. There are two differences to point out between these two setups. First, the deformation stress states of the straight groove test may differ to the conical shapes formed here. Literature has shown that with increasing ratio of shape curvature to tool diameter, greater plane strain conditions are observed [39]. As the ratio decreases, the deformation strain becomes more biaxial in nature. Second, in UA-ISF, the ultrasonic effects exist in both surface and volume region of the sheet, which are reflected as friction and flow stress reduction respectively. The repeated deformation of the same area of material in Vahdati's line test can potentially optimize on volume effects of the previous pass. During the process of forming conical shapes in this study, new material is being deformed. However, with finer step sizes, we do observe increases in force reduction but this current data set has only two varying step sizes. Interactions between the tool's current path and previous path requires further study and a larger sample size. In addition, their forming forces did not appear to have large dips which may be an influence of the geometry and the forming area opening of their groove test. Further membrane modelling study will be needed to determine if the tool passes over resonance locations since the sheet geometry continuously changes during incremental forming, which can modify the natural vibration frequency of the sheet.

The relationship between oscillation amplitude and force reductions is consistent with the results of fundamental studies on ultrasonic assisted tensile and compression tests [22,23]. As the oscillation amplitude increases, the force reduction increases as shown in Fig. 5 and Fig. 6. The variation in thickness of UASPIF samples were within the error of the scanning tool, 0.063mm, and therefore we cannot conclude that there are any significant changes in the thickness due to UA during SPIF.

4.2 Effect of ultrasonic vibrations on two-point incremental forming

In comparison to UA-SPIF, the force reduction in UA-TPIF is considerably higher. As seen in Fig. 9 and Fig. 10, when UA is turned on the axial force drops and asymptotes to a lower average value. The planar force approaches a lower mean value but more gradually. There are two distinctions between the 0.5mm and 0.25mm step size UA-TPIF samples. First, both axial and planar force reductions are higher for the smaller step size sample at equal programmed squeeze and angle. This requires further study as the experiments presented here only involve two levels of step size. The second observation is the appearance of a transient behavior in the 0.25mm step size sample. Both regions R2 and R3 show transient behavior when UA is turned on and off which correlates to the transient thickness behavior in Fig. 10. Additional tests are required to determine if the steady state value is coincidentally due to the period of this ultrasonic cycle or the inherent forming behavior regardless of the UA period.

Ultrasonic vibration has the potential to heat the material and lower the flow stress. However, increases in temperature have been found, in tensile and compression tests, to be negligible and only occur with large acoustic intensities [27,33, 40]. In addition, during ultrasonic-assisted compression and tension tests, the ultrasonic vibrations are applied to the entire specimen continuously. In comparison, during UA-ISF, new material is continuously being deformed under the tool. As such, the effect of temperature on flow stress reductions was assumed to be negligible in this work.

The corresponding thickness profile of the formed sheet is shown in Fig. 10. Once the UA is turned on, the sheet thickness decreases and reaches a minimum value of 0.97mm in region R2 with the current set of process parameters. After UA is turned off, the thickness gradually increases to a value greater than the minimum thickness in region R1. Assuming conservation of volume, the material in the thinned region would have had to be pushed towards the center of the part, which is indicated by a larger thickness in region R3. The difference in minimum thickness between region R1 and R2 is 150μm for a tool oscillation amplitude of only 3.29μm. This difference can be noticed visually from Fig. 11.

This study provides preliminary results into the effects of applying ultrasonic vibrations in both single-point and two-point incremental sheet forming. Additional experiments are planned as only one part was formed for each process parameter in this study. Further work is required to understand transient behaviors and the effect of step size on force and thickness reduction.

5. Conclusions

In this study, AA 7075-O sheet samples were incrementally formed under ultrasonic assistance in single and two-point incremental configurations. Based on the measured forming forces and thickness values, following conclusions can be made:

- Ultrasonic vibration can reduce forming forces during incremental forming process.
- Reduced axial and planar forming forces were observed in both UA-TPIF and UA-SPIF process under different forming angles and incremental step sizes.
- The magnitude of force reductions generally increases as the oscillation amplitude increases.
- The magnitude of force reduction is significantly larger for UA-TPIF compared with UA-SPIF. The smaller force reduction in SPIF is hypothesized to be due to energy transferred to membrane vibration.
- When UA is turned on during UA-TPIF, a force reduction is seen in both the axial and planar curve. The observed thickness reduction is much higher than the oscillating displacement amplitude of the tool.

Acknowledgements

The authors would like to acknowledge the National Science Foundation (CMMI No. 1841755) and Light Weight Innovations for Tomorrow (LIFT) (DOD-ONR N00014-14-2-0002- LIFT 0007A-4) for their support.

References

[1] Jackson, K., and Allwood, J., 2009, "The mechanics of incremental sheet forming," Journal of materials processing technology, 209(3), pp. 1158-1174.

[2] Malhotra, R., Xue, L., Belytschko, T., and Cao, J., 2012, "Mechanics of fracture in single point incremental forming," Journal of Materials Processing Technology, 212(7), pp. 1573-1590.

[3] Brosius, A., 2014, "Incremental Forming," CIRP Encyclopedia of Production Engineering, L. Laperrière, and G. Reinhart, eds., Springer Berlin Heidelberg, Berlin, Heidelberg, pp. 689-692.

[4] Baghlani, V., Mehbudi, P., Akbari, J., and Sohrabi, M., 2013, "Ultrasonic assisted deep drilling of Inconel 738LC superalloy," Procedia CIRP, 6, pp. 571-576.

[5] Chen, C., Cui, C., Zhao, L., Liu, S., and Liu, S., 2016, "The formation mechanism and interface structure characterization of in situ AlN/Al composites," Journal of Composite Materials, 50(4), pp. 495-506.

[6] Shen, X.-H., Zhang, J., Xing, D. X., and Zhao, Y., 2012, "A study of surface roughness variation in ultrasonic vibration-assisted milling," The International Journal of Advanced Manufacturing Technology, 58(5-8), pp. 553-561.

[7] Murakawa, M., and Jin, M., 2001, "The utility of radially and ultrasonically vibrated dies in the wire drawing process," Journal of Materials Processing Technology, 113(1-3), pp. 81-86.

[8] Jimma, T., Kasuga, Y., Iwaki, N., Miyazawa, O., Mori, E., Ito, K., and Hatano, H., 1998, "An application of ultrasonic vibration to the deep drawing process," Journal of Materials Processing Technology, 80, pp. 406-412.

[9] Hung, J.-C., and Hung, C., 2005, "The influence of ultrasonic-vibration on hot upsetting of aluminum alloy," Ultrasonics, 43(8), pp. 692-698.

[10] Mousavi, S. A., Feizi, H., and Madoliat, R., 2007, "Investigations on the effects of ultrasonic vibrations in the extrusion process," Journal of materials processing technology, 187, pp. 657-661.

[11] Gallego-Juárez, J. A., and Graff, K. F., 2014, Power ultrasonics: applications of high-intensity ultrasound, Elsevier.

[12] Kumar, V. C., and Hutchings, I. M., 2004, "Reduction of the sliding friction of metals by the application of longitudinal or transverse ultrasonic vibration," Tribology International, 37(10), pp. 833-840.

[13] Perotti, G., "An experiment on the use of ultrasonic vibrations in cold upsetting," Proc. CIRP Annales, pp. 195-197.

[14] Pohlman, R., and Lehfeldt, E., 1966, "Influence of ultrasonic vibration on metallic friction," Ultrasonics, 4(4), pp. 178-185.

[15] Bunget, C., and Ngaile, G., 2011, "Influence of ultrasonic vibration on micro-extrusion," Ultrasonics, 51(5), pp. 606-616.

[16] Amini, S., Gollo, A. H., and Paktinat, H., 2017, "An investigation of conventional and ultrasonic-assisted incremental forming of annealed AA1050 sheet," The International Journal of Advanced Manufacturing Technology, 90(5-8), pp. 1569-1578.

[17] Vahdati, M., Mahdavinejad, R., and Amini, S., 2017, "Investigation of the ultrasonic vibration effect in incremental sheet metal forming process," Proceedings of the Institution of Mechanical Engineers, Part B: Journal of Engineering Manufacture, 231(6), pp. 971-982.

[18] Blaha, F., and Langenecker, B., 1955, "Tensile deformation of zinc crystal under ultrasonic vibration," Naturwissenschaften, 42(556), p. 0.

[19] Siddiq, A., and El Sayed, T., 2011, "Acoustic softening in metals during ultrasonic assisted deformation via CP-FEM," Materials Letters, 65(2), pp. 356-359.

[20] Siddiq, A., and Ghassemieh, E., 2008, "Thermomechanical analyses of ultrasonic welding process using thermal and acoustic softening effects," Mechanics of Materials, 40(12), pp. 982-1000.

[21] Yao, Z., Kim, G.-Y., Wang, Z., Faidley, L., Zou, Q., Mei, D., and Chen, Z., 2012, "Acoustic softening and residual hardening in aluminum: Modeling and experiments," International Journal of Plasticity, 39(Supplement C), pp. 75-87.

[22] Lum, I., Huang, H., Chang, B., Mayer, M., Du, D., and Zhou, Y., 2009, "Effects of superimposed ultrasound on deformation of gold," Journal of Applied Physics, 105(2), p. 024905.

[23] Zhou, H., Cui, H., and Qin, Q. H., 2018, "Influence of ultrasonic vibration on the plasticity of metals during compression process," Journal of Materials Processing Technology, 251, pp. 146-159.

[24] Huang, H., Pequegnat, A., Chang, B., Mayer, M., Du, D., and Zhou, Y., 2009, "Influence of superimposed ultrasound on deformability of Cu," Journal of Applied Physics, 106(11), p. 113514.

[25] Siddiq, A., and El Sayed, T., 2012, "A thermomechanical crystal plasticity constitutive model for ultrasonic consolidation," Computational Materials Science, 51(1), pp. 241-251.

[26] Langenecker, B., 1966, "Effects of Ultrasound on Deformation Characteristics of Metals," IEEE Transactions on Sonics and Ultrasonics, 13(1), pp. 1-8.

[27] Siu, K. W., Ngan, A. H. W., and Jones, I. P., 2011, "New insight on acoustoplasticity – Ultrasonic irradiation enhances subgrain formation during deformation," International Journal of Plasticity, 27(5), pp. 788-800.

[28] Siu, K. W., and Ngan, A. H. W., 2011, "Understanding acoustoplasticity through dislocation dynamics simulations," Philosophical Magazine, 91(34), pp. 4367-4387.

[29] Dutta, R., Petrov, R., Delhez, R., Hermans, M., Richardson, I., and Böttger, A., 2013, "The effect of tensile deformation by in situ ultrasonic treatment on the microstructure of low-carbon steel," Acta Materialia, 61(5), pp. 1592-1602.

[30] Malygin, G., 2000, "Acoustoplastic effect and the stress superimposition mechanism," Physics of the Solid State, 42(1), pp. 72-78.

[31] Nevill, G. E., 1957, "Effect of vibrations on the yield strength of a low carbon steel," PHD Thesis, Rice University.

[32] Kirchner, H. O. K., Kromp, W. K., Prinz, F. B., and Trimmel, P., 1985, "Plastic deformation under simultaneous cyclic and unidirectional loading at low and ultrasonic frequencies," Materials Science and Engineering, 68(2), pp. 197-206.

[33] Daud, Y., Lucas, M., and Huang, Z., 2007, "Modelling the effects of superimposed ultrasonic vibrations on tension and compression tests of aluminium," Journal of Materials Processing Technology, 186(1), pp. 179-190.

[34] Maya Nath, J., Ankush Bansal, Mihaela Banu, Alan Taub, 2018, "Comparison of Texture and Surface Finish Evolution During Single Point Incremental Forming and Formability Testing of AA 7075," Light Metals 2018, The Minerals, Metals & Materials Series, Accepted.

[35] Salem, E., Shin, J., Nath, M., Banu, M., and Taub, A. I., 2016, "Investigation of Thickness Variation in Single Point Incremental Forming," Procedia Manufacturing, 5, pp. 828-837.

[36] Jeswiet, J., Micari, F., Hirt, G., Bramley, A., Duflou, J., and Allwood, J., 2005, "Asymmetric Single Point Incremental Forming of Sheet Metal," CIRP Annals, 54(2), pp. 88-114.

[37] Nath, M., Shin, J., Bansal, A., Banu, M., and Taub, A., "Comparison of Texture and Surface Finish Evolution During Single Point Incremental Forming and Formability Testing of AA 7075," Proc. TMS Annual Meeting & Exhibition, Springer, pp. 225-232.

[38] Morse, P. M., and Ingard, K. U., 1968, Theoretical acoustics, Princeton university press.

[39] L. Filice, L. Fratini, and F. Micari, “Analysis of Material Formability in Incremental Forming,” CIRP Ann., vol. 51, no. 1, pp. 199–202, Jan. 2002.

[40] T. Liu, J. Lin, Y. Guan, Z. Xie, L. Zhu, and J. Zhai, “Effects of ultrasonic vibration on the compression of pure titanium,” *Ultrasonics*, vol. 89, pp. 26–33, Sep. 2018.